Improved Signal Processing Methods for Velocity Selective Neural Recording Using Multi-Electrode Cuffs

Assad Al-Shueli, Chris Clarke, Nick Donaldson and John Taylor

***Abstract*—This paper describes an improved system for obtaining velocity spectral information from *electroneurogram* recordings using *multi-electrode cuffs* (MECs). The starting point for this study is some recently published work that considers the limitations of conventional linear signal processing methods ('delay-and-add') with and without additive noise. By contrast to earlier linear methods, the present paper adopts a fundamentally non-linear *velocity classification* approach based on a type of artificial neural network (ANN). The new method provides a unified approach to the solution of the two main problems of the earlier delay-and-add technique, i.e. a damaging decline in both *velocity selectivity* and *velocity resolution* at high velocities. The new method can operate in real-time, is shown to be robust in the presence of noise and also to be relatively insensitive to the form of the action potential waveforms being classified.**

***Index Terms*— Biomedical signal processing, Biomedical transducers, Microelectronic implants, Neural prosthesis, Artificial neural networks**

I. Introduction

One component of neuroprosthetic systems is the neural input through which information is transferred from a physiological environment into the prosthesis. Tripolar recording from peripheral nerves cannot generally extract much of the information in the neural traffic, so we and others have been investigating *velocity selective recording* (VSR) since it allows the possibility of increasing the information obtainable from peripheral nerves (*electroneurogram*-ENG) by carrying out a spectral analysis in the *velocity* domain [1]-[7]. The resulting spectrum shows not only the direction of *action potential* (AP) propagation (*afferent* or *efferent*) but also provides a measure of the differential levels of excitation of the fibre populations in the nerve. Since there is a well-established relationship between AP propagation velocity and fibre diameter that is approximately linear for *myelinated* fibres, VSR provides a method for assessing the level of activity in nerve fibre populations of different diameter as well as establishing the direction of propagation. This information potentially allows more information to be extracted from an intact nerve for use in applications requiring sensory feedback such as neuroprostheses [8]-[11].

TABLE I
A List of Acronyms Used

Acronym	Meaning
ADC	Analogue to Digital Converter
ANN	Artificial Neural Network
AP	Action Potential
FPGA	Field Programmable Gate Array
IVS	Intrinsic Velocity Spectrum
MEC	Multi-Electrode Cuff
SNR	Signal to Noise Ratio
SPU	Signal Processing Unit
TMAP	Trans-Membrane Action Potential
VSR	Velocity Selective Recording

In principle the velocity of a propagating AP can be calculated by timing the appearance of the signal at two or more points along the nerve and then dividing the distance between the points by the delay. Various researchers have investigated practical adaptations of this simple idea in the past (e.g. [12]-[14]). These methods were made both possible and practical by the introduction of electrode cuffs in 1974-75 [15] that provided for the first time a stable, chronically implantable interface for both neural stimulation and recording. However, each cuff contained typically only 2-3 electrodes limiting the available velocity selectivity. The invention of the multi-electrode cuff (MEC) [16] has been very influential in improving this situation, enabling recordings to be made with increased velocity selectivity (each MEC contains typically about 10-15 electrodes). Using this approach it should be possible to access slower (i.e. smaller diameter) fibres than was the case with the earlier, simpler cuffs whilst at the same time offering the potential for incorporation in compact, integrated implantable systems. In addition, considerable progress has been made in the design of implantable integrated signal processing systems featuring low-noise, low-power amplifiers intended to be mounted directly on the MEC for optimum signal-to-noise performance [2], [3].

The method currently in use to estimate the velocity spectrum of ENG data captured by an MEC-based system is based on linear signal processing principles and is referred to

Manuscript received April 21, 2013. This work was supported in part by the European Union under IMANE (IST-026602).

Chris Clarke is with the Department of Electronic and Electrical Engineering, University of Bath, UK (phone: +44-1225-386322; fax: +44-1225-386305; e-mail: c.t.clarke@bath.ac.uk).

John Taylor is with the Department of Electronic and Electrical Engineering, University of Bath, UK (e-mail: j.t.taylor@bath.ac.uk).

Assad Al-Shueli is with the Department of Electronic and Electrical Engineering, University of Bath, UK (e-mail: a.i.k.al-shueli@bath.ac.uk).

Nick Donaldson is with Department of Medical Physics and Bioengineering, University College London, UK (e-mail: nickd@medphys.ucl.ac.uk).

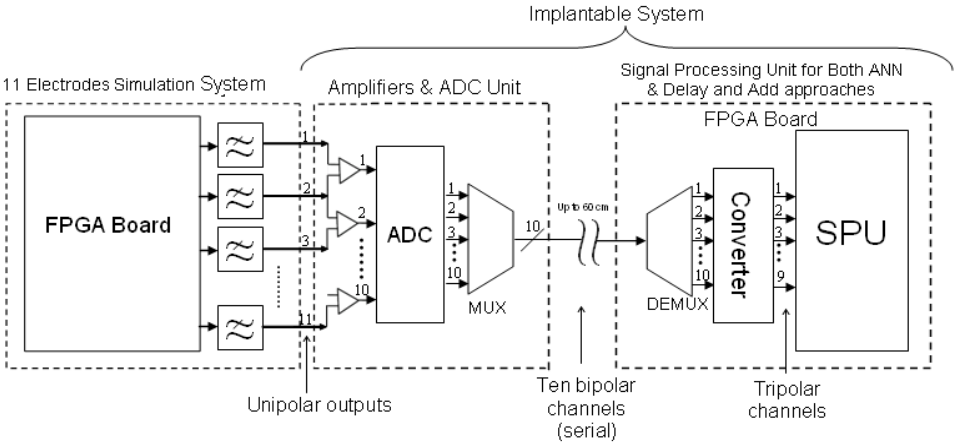

Fig. 1. Block diagram of the complete system consisting of three units as indicated by the dashed boxes. The first box on the left is an 11-channel action potential (AP) synthesiser that provides the input to the second stage which is a signal acquisition, digitisation and serialisation block. This is a CMOS ASIC intended for implantation. The resulting 10 digitised and serialised bipolar channels are finally processed on an FPGA board that allows a convenient comparison of the various classification methods (ultimately this part of the system will also be implemented as an ASIC).

as 'delay-and-add'. The resulting profile of relative signal output as a function of velocity is called the intrinsic velocity spectrum (IVS) [2]. There are two main problems with this approach, however. Firstly, the IVS provides limited velocity selectivity, especially at higher velocities (this is mostly because the maximum length of an implantable MEC is set by surgical constraints to about 3 cm). Secondly, the precision with which the velocity spectral components can be specified (velocity resolution) declines at high propagation velocities due to a combination of the fundamental nature of the process and the practical effect of finite sampling rates. In order for VSR recording to work effectively, both problems must be solved.

In this paper we propose a nonlinear approach based upon a type of artificial neural network (ANN) to tackle both the difficulties mentioned above without increasing either the length of the MEC or the sampling rate. It is shown that good results can be achieved with a very simple optimized non-linear system (although we retain the term ANN due to the training methods used in the optimization). In addition, the new method achieves significantly higher velocity selectivity than any other currently available method and since it requires supervised learning, once trained it runs in real-time. Although ANNs have been employed in related applications (e.g. AP classification [17]) this is the first time they have been proposed as a method to discriminate between the velocities of propagating ENG. The approach is somewhat analogous to that employed in speech recognition and hence the chosen type of ANN, a time-delay neural network, was first employed in that application [18]. This paper consists of a study based on ENG data generated using a specially designed synthesised source [19] that permits the addition of controlled amounts of white Gaussian noise. The behaviour of the ANN-based velocity classifier is examined as the noise level is increased and the form of the AP input is varied from the pattern used for training. The results are compared to the performance of a 'conventional' delay-and-add system. Finally, the hardware cost of an ANN-based classifier relative to an equivalent delay-and-add system is assessed.

II. Methods

A. System Description

1) Conventional VSR signal processing: 'delay-and-add'

The overall plan of the complete system is shown in Fig 1 and consists of three separate stages. The first stage on the left (block 1) is an FPGA-based programmable AP and noise signal generator (synthesiser) whose output is eleven *unipolar* signals delayed so as to simulate an AP moving through the cuff [19]. The signals are generated using a modified pulse-width modulation output direct from the FPGA. In this study we consider an MEC of length 3 cm and propagation velocities in the range 10 – 100 m/s although operation at lower velocity is also possible. To these signals controlled amounts of uncorrelated additive white Gaussian noise were added [3]. Blocks 2 and 3 are the two principal sections of a neural recording system intended for ultimate implantation as a pair of remotely powered modules connected together using a multicore implantable cable [7]. Block 2 is referred to as the *electrode unit* and is intended to be mounted on the MEC for optimum performance. It consists of a set of specially-designed low noise differential amplifiers (nominal gain 10,000) whose 10 *bipolar* (or single differential) outputs are digitized (10 bits resolution) and multiplexed into one channel for transmission along the implantable cable [6]. In a distributed sensor architecture, several electrode units are placed at different sites in the peripheral nervous system and connected by implanted cables to a single *monitoring unit* [7]. The monitoring unit is a demultiplexer (DEMUX) and digital signal processing system that interfaces with an RF telemetry system (not described in this paper). In addition to processing and transmitting the recorded data for external logging, the monitoring unit processes the system commands and provides power supplies.

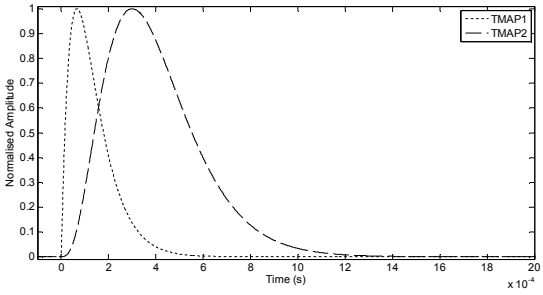

Fig. 2. The TMAPs used in this paper are based upon equation (1) with different parameters. TMAP1 is used throughout this paper except where noted otherwise.

Although a single monitoring unit can process the data from and control and power several electrode units [7], in the experiments described in this paper only one of each type of unit is used as shown in Fig 1. In addition, the electrode unit employed is a complete prototype custom integrated circuit whereas the monitoring unit is realised in FPGA. Although for ultimate implantation the monitoring unit will be a second integrated circuit, the comparison of different VSR signal processing strategies that lies at the heart of this investigation requires easy flexibility of design suggesting the use of FPGA. The signal processing circuitry is contained in the unit on the far right of block 3 in Fig 1 (SPU) and is preceded by stages of de-multiplexing into 10, parallel bipolar channels and conversion into 9 *tripolar* (or double differential) channels. Tripolar signals are generally employed in ENG recording applications since they have enhanced immunity to common mode signal contamination (such as *electromyogram*) compared to monopolar or bipolar ones [20]. Finally the captured and recorded signals are processed in MATLAB. As already noted, the fundamental comparison to be made is between the conventional delay-and-add method [1] and the proposed new method, which employs an ANN as the core of the SPU.

2) Action potential (AP) and noise generation

The AP generator was described in [19] and so only a summary will be given here. The input to the MEC is a *trans-membrane action potential* function (TMAP), $V_m(t)$ and the resulting single fibre action potential is a propagating wave with the time dependence of the underlying TMAP function and the spatial properties of the MEC [2]. The TMAP can therefore be regarded as the driving potential resulting in a propagating electric field. APs appear at electrodes placed in this field. We represent the TMAP function by the following time-varying function [1]:

$$V_m(t) = At^n e^{-Bt} \quad (1)$$

where A, B and n are constants. These constants are chosen to generate APs with typical mammalian shape, the duration of the resulting signals being on the order of 1 ms. In this paper we use one of the TMAP functions that formed the basis of the analysis in [2]. The parameter values in eqn (1) are: A = 4.08 x 10^{-3}, B = 1.5 x 10^4 and n = 1. In section III C a second function (TMAP2) is introduced as an example of other

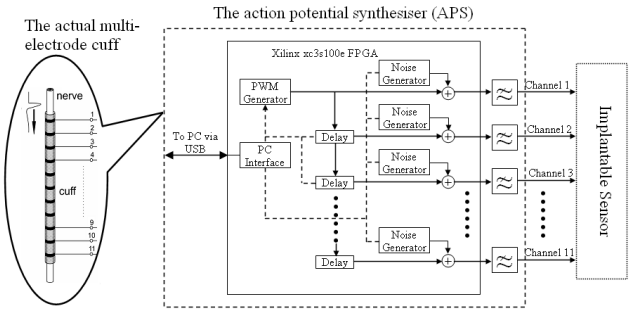

Fig. 3. Simplified block diagram of the action potential synthesiser (APS) with programmable inter-electrode delay and action potential (AP) shape. The action potential synthesiser is connected directly to the implantable sensor and provides it with the signals that would be expected if the actual multi-electrode cuff were connected in an in-vitro experiment. Extra circuitry is provided within the synthesiser for the addition of controlled amounts of white Gaussian noise.

parameter sets that can also be used. The signal TMAP2 is used to investigate the effect of varying the TMAP on the performance of the system. In this case the parameters are: A = 7.44 x 10^{-11}, B = 1.0 x 10^4 and n = 3. The form of both of these functions is shown in Fig 2.

The AP signal generation system is implemented as an FPGA controller plus a few passive components. It employs pulse-width modulation and related methods to achieve a very smooth representation of $V_m(t)$ without the need for excessively high sample rates and/or high resolution digital components[19]. For the purposes of this study, the system is modified to allow variable amounts of noise to be added to each channel. Linear feedback shift registers with different tap positions were added to provide the necessary uncorrelated noise sources, the noise level being controlled by an 8-bit counter and a comparator. The controller has a USB interface to a desktop PC that allows easy programmability of all the main parameters. A simplified block diagram of the AP generator is given in Fig 3 showing the modifications necessary for the inclusion of noise.

B. VSR Signal Processing Methods

1) Conventional VSR signal processing: 'delay-and-add'

Fig 4 is the block diagram of the signal-processing unit

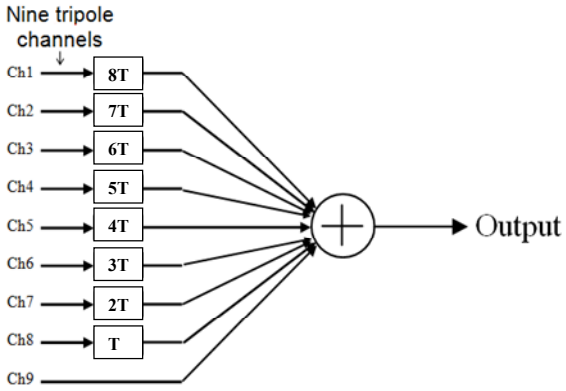

Fig. 4. Signal processing unit (SPU) for the conventional linear ('delay-and-add') VSR method.

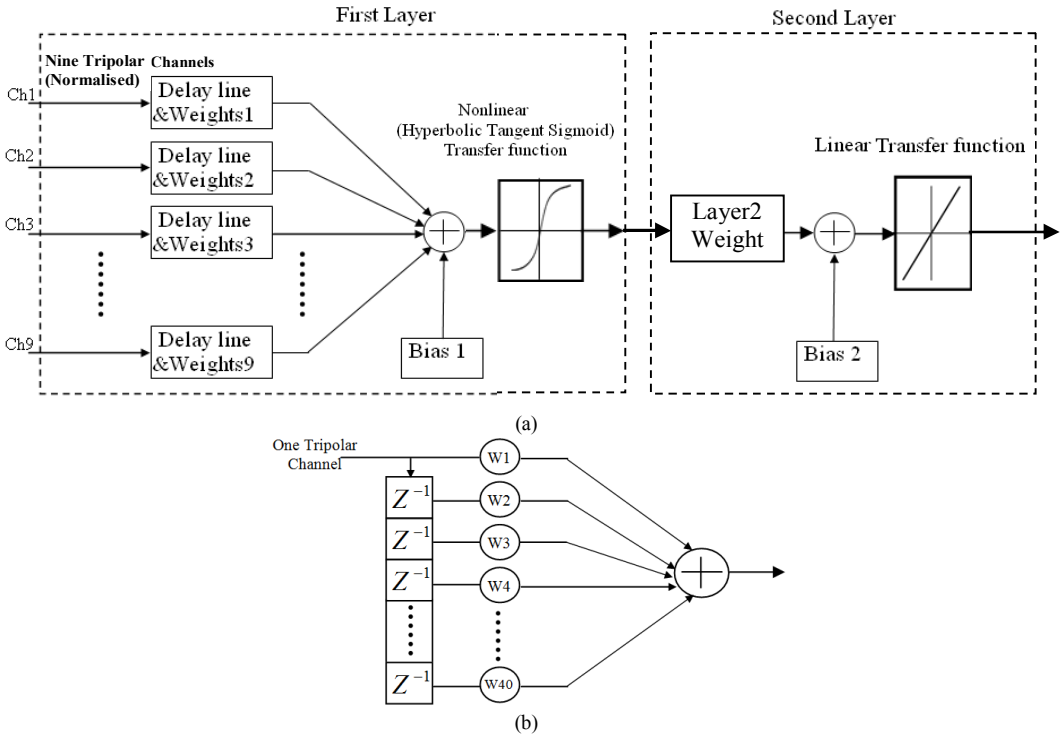

Fig. 5. (a) modified signal processing unit (SPU) using ANN-based methods, consisting of two layers. The first layer has nine tripole inputs each of which is connected to a tapped delay line (FIR filter) with adaptive weights. The outputs of the delay lines are summed to a single channel and passed through a non-linear gain stage forming the input to layer 2. Layer 2 consists of a single adaptive weight and bias followed by a linear gain stage. Detail of single delay line with adaptive weights unit is given in (b).

(SPU) in a conventional VSR system. One complete set of fixed delays is required for each AP propagation velocity to be classified [2]. In an implanted system the SPU will be connected to the mixed analogue/digital signal acquisition integrated circuits by means of implanted cables and so, as already noted, the multiplexed input is first de-multiplexed into 10 parallel (dipole) channels. After the signals are converted to tripolar form, the next steps are to add programmable delays to counteract the naturally- occurring delays and then sum the outputs. In the presence of an excited population with propagation velocity v, as the delays are stepped through the appropriate range, the output passes through a maximum when the delay T is given by:

$$T = d/v \qquad (2)$$

where d is the inter-electrode spacing. There are two fundamental problems with this approach, however. Firstly, for a practical cuff length (i.e. about 2-3 cm) the available velocity selectivity is generally too low to be useful. This issue can be mitigated to some extent by placing bandpass filters at the output [2]. Secondly, the *velocity resolution*, that is to say the number of available points on the velocity axis, declines at high velocities making the velocity spectral content difficult to measure. This is because the inter-channel delays (T) generated by a typical MEC are small at high velocities which limits the number of possible velocity steps. Since the relationship between delay and velocity is reciprocal (see eqn 2) the available points are concentrated at low velocities, leaving few higher up the scale. For example, for an MEC where d = 3 mm, for v = 100 m/s, from eqn (2), T = 30 µs, i.e. about one sample period. So in this case an inter-electrode delay of 1 sample period corresponds to a velocity of 100 m/s, 2 samples delay represents 50 m/s, with no possible velocity values between the two.

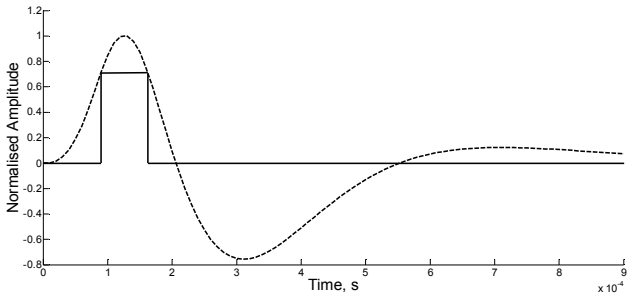

Fig. 6. A typical *tripolar* action potential (AP) illustrating the derivation of a rectangular pulse of the type used as one of the training targets for the ANN. The pulse is fitted to the positive phase of the AP, the amplitude and duration of the pulse being chosen to reflect the points at which the amplitude of the AP has fallen to 3 dB below its peak value.

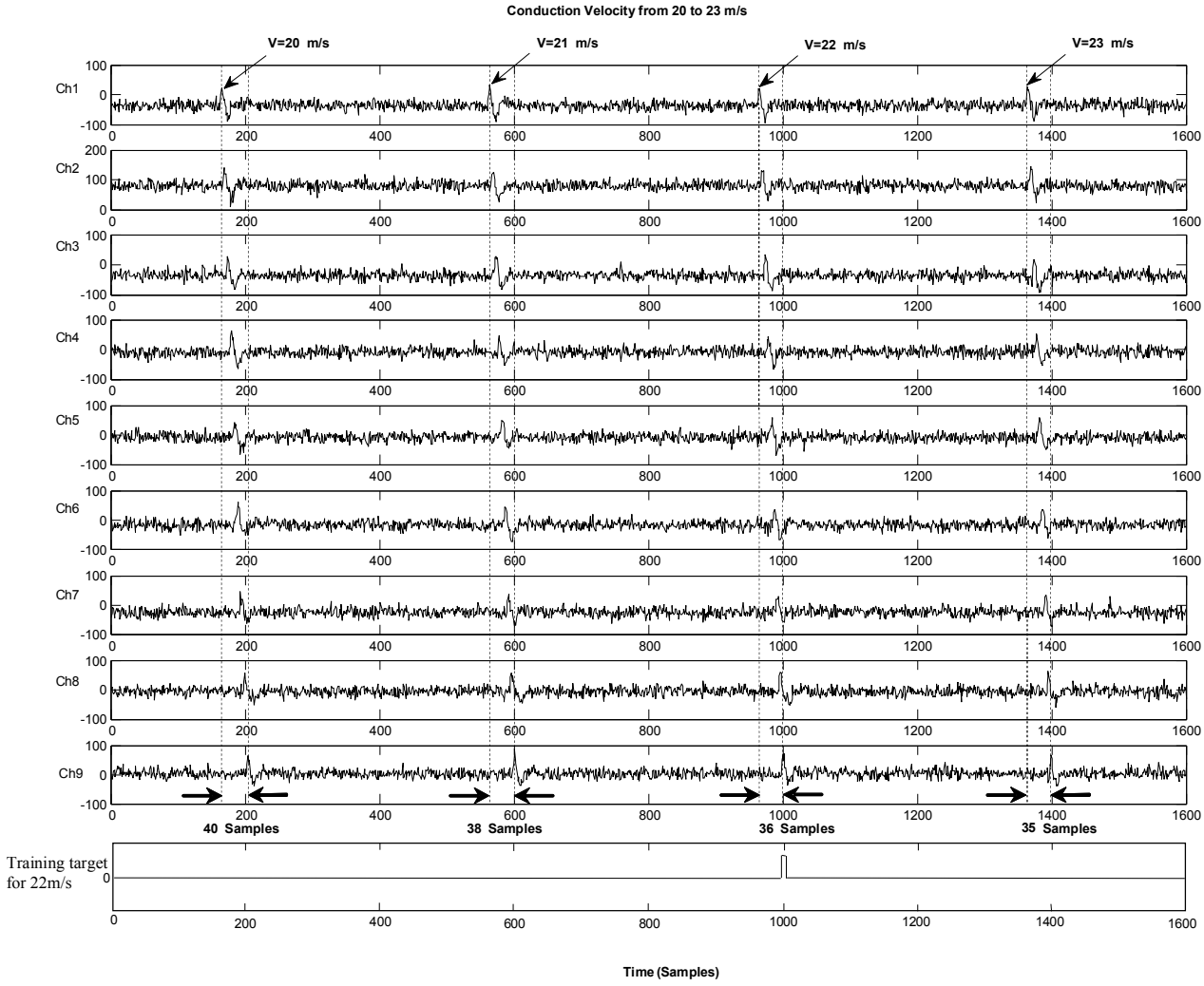

Fig. 7. A section of tripolar training data with APs that are 400 samples apart, corresponding to a duration of 12ms. This allows for the maximum delay encountered by an AP in this system (1.2ms). The section contains four APs with propagation velocities of 20, 21, 22 & 23 m/s and the SNR is 1 in all cases. For the system shown here, the MEC has 11 electrodes with 3mm separations and the signal is sampled at 32.5 kSa/s. The signals Ch1 to Ch9 correspond to tripolar signals from the 11 unipolar signals of the MEC as shown inset in Fig 2. The target shown is that required for training the ANN to detect APs with velocities of 22 m/s. In the full training sequence, this target amplitude is zero throughout the rest of the training sequence whilst the AP velocities increase to 120m/s.

Tuning curves were introduced as a compact method to display the velocity spectral behavior of a VSR system by analogy to techniques familiar from the frequency domain analysis of linear systems [1]. The magnitude of the output of the system is plotted as a function of velocity and so the method is somewhat analogous to computing the frequency response of a linear system. This analogy has been expanded to propose a metric Q_v to quantify velocity selectivity, the idea being based on the *quality factor* familiar from the study of linear resonant circuits [3]. Q_v is defined as $v_0/(v_{3+}-v_{3-})$ where v_0 is the matched velocity. v_{3+} and v_{3-} are the velocities where the normalized amplitude of the tuning curve drops to $1/\sqrt{2}$ either side of the matched velocity (v_{3+} above and v_{3-} below). More recently, an additional parameter, R_v, has been introduced in an attempt to quantify velocity resolution [6]. R_v is defined as $\Delta v/v$, where Δv is minimum available velocity step at propagation velocity v. It was suggested in [6] that a reasonable maximum value for R_v across the velocity band of interest would be about 0.1. For example, with the values in the previous paragraph, at a propagation velocity of 10 m/s, R_v = 0.11, which is satisfactory, but at 100 m/s, this has risen to 0.5, which is clearly not. These parameters are employed in the analysis and comparison of systems in the following paragraphs.

It has been shown that the first problem (low velocity selectivity) can be resolved by placing bandpass filters at the output of the system [2]. However without a solution to the resolution issue, this would be ineffective since no data at high velocities can be recorded. Conversely, although the resolution problem can be solved using some form of interpolation, this does not improve the situation at high velocities if the underlying selectivity is inadequate. In the next section we propose an alternative process to delay-and-add that offers an effective solution to both problems.

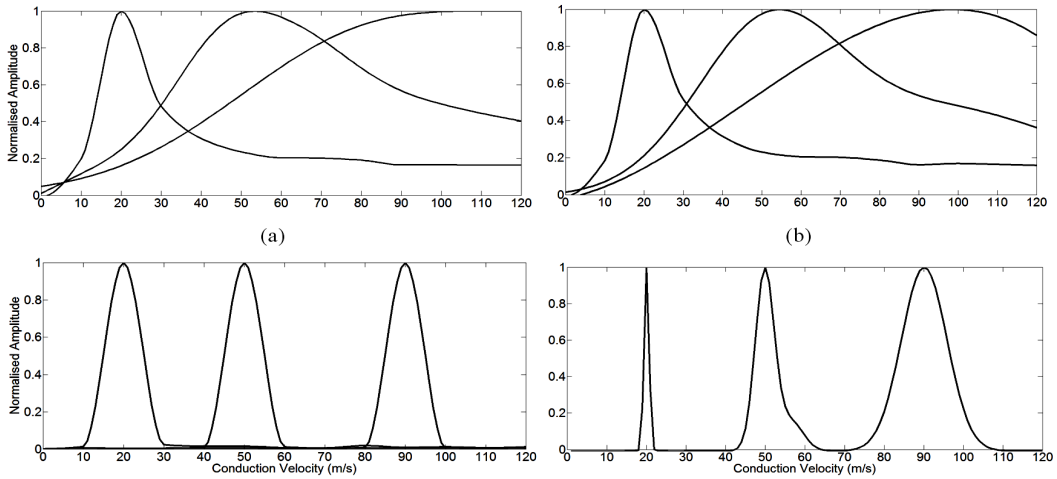

Fig. 8. Tuning curves comparing the characteristics of the methods under consideration in the absence of noise for matched velocities of 20, 50 and 90m/s. Fig 8(a) and (b) show the results for standard delay-and-add matching with (b) and without (a) interpolation. Figs 8(c) and (d) show the results using an ANN classifier with AP and pulse training respectively. For the 50 m/s curve, the velocity Q factors (Qv) are 1.2 for (a) and (b), 7.1 for (c) and 12.5 for (d).

2) Artificial neural network method for VSR

Figure 5 shows the network structure used in this study. The network selected is a feed-forward type, specifically a *time-delay neural network*. As already noted this network has been applied in analogous applications such as speech recognition [18] and time series prediction [21]. As in the case of the delay-and-add method, one complete structure is required for each velocity to be classified. As in Fig 4, the inputs to the ANN derive from the outputs of the DEMUX but in this case the inputs are normalised (variable spike amplitudes are a potential issue in assessing the performance of the ANN but have not been considered in this study). Each of the nine *tripolar* output channels ($1 \leq i \leq 9$) forms the input to a shift register whose outputs are multiplied by a set of programmable weights w_{ij}. The length of the shift registers is determined by the maximum required delay and this is set by the minimum velocity to be considered (in this case 10 m/s) and the inter-electrode spacing, d. Using eqn (2) with d = 3 mm, the corresponding inter-channel delay at this velocity is 150 μs or 1.2 ms for the complete 9 channel tripolar system. For a sampling period T_s of 30 μs, each shift register therefore requires 40 stages ($1 \leq j \leq 40$) and hence for each training set a matrix of (9 x 40) weights is computed and stored. The output consists of the sum of 9 overlaid weighted sets of 40 samples each, the values at each sample point being different from set to set reflecting the time shift along the MEC. The summed output is then passed through a second layer consisting of a single neuron, which is realised as a linear or nonlinear (Hyperbolic Tangent Sigmoid) function.

3) ANN training method

The time-delay neural network requires supervised learning using pre-determined *targets* after which the system can be run in real-time. Two types of target were tested: (i) a complete tripolar AP scaled appropriately for d and v (see eqn 2 and [2]) and (ii) a rectangular pulse derived from the AP. The pulse width and amplitude of the pulse target were derived from the positive phase of the AP at the points where its amplitude had fallen below the peak value by 3 dB, as illustrated in Fig 6. The pulse therefore expresses the delay, amplitude and duration of the AP. The recording duration required to capture the entire transit of an AP through the cuff is a function of propagation velocity, the electrode spacing d, the number of electrodes and the TMAP function itself. The pulse as derived expresses the propagation velocity since the other parameters are constants. For the training process itself, a set of 9 *tripolar* input signals of normalised amplitude are applied in parallel and the summed output is then compared to the target waveform generated from the analytical TMAP model function (eqn (1)) as described above. The input signals are generated by the synthesiser, which, as already noted, adds noise to each channel as required.

Each of the records from the 9-tripolar channels is divided into time segments and each segment contains a single AP of normalised amplitude propagating at a particular velocity. For a complete set of 9 segments the relative delays between the pulses define the unique propagation velocity of the AP in each segment. Note that the minimum length of the segments is set by the total length of 9 APs delayed to represent the slowest propagation velocity under consideration. For example, in the cases considered in this paper, the data were sampled at f_s = 32.5 kSa/s. For a typical 3 cm separation between the end-electrodes of the MEC and a minimum AP velocity of 20m/s the delay is 1.2 ms (8 times T). The chosen delay line length of 40 samples (corresponding to a duration of 1.2 ms) is therefore more than adequate for the full range of propagation velocities under consideration. Fig 7 shows four example time segments taken from the training set to which noise was added (signal-to-noise ratio (SNR) = 1-see below). The tripolar APs in these segments have propagation velocities ranging from 20 to 23 m/s.

The summed output is compared to the target representing one velocity and coincident with the final (i.e. the most delayed) channel input at the matched velocity. At all other times the target amplitude is zero. The difference between the

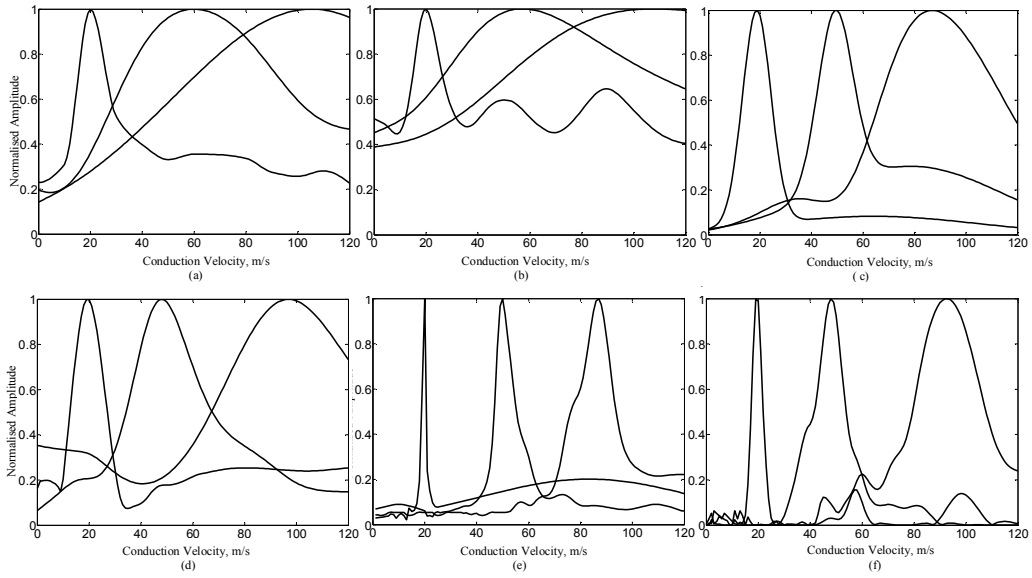

Fig. 9. Tuning curves with additive white Gaussian noise for signal-to-noise ratios of 1 and 0.1 respectively for conduction velocities of 20, 50 and 90 m/s. Graphs a & b show the interpolated delay-and-add method while the graphs c & d and graphs e & f are for the ANN trained with the complete AP and pulse targets respectively. At 50 m/s and SNR = 1, for delay-and-add, Q_v = 1.1. For the ANN, Q_v = 3.8 (AP target) and 10.0 (pulse target). Corresponding values for SNR = 0.1 are: 0.6, 2.3 and 6.3, respectively.

training data and the template forms the basis of the back-propagation training process [22], [23]. Note that the designer can effectively choose the scale on the velocity axis as part of the training process, to some extent removing the problem of reduced velocity resolution at high propagation velocities encountered by the delay-and-add method.

III. Results

A. Noiseless tuning curves

As an initial step, the system was set up to detect *three* velocities in the appropriate range (20 m/s, 50 m/s and 90 m/s). This requires three networks of the type shown in Fig 4 (for delay-and-add) or Fig 5 (for ANN), one for each target velocity. Tuning curves were then computed for each trained velocity [1]. The results are shown in Fig 8. Figs 8(a) and (b) show the outputs obtained using the conventional linear delay-and-add method and display the characteristic difficulties of this approach as described above in Section II.B.1 (Conventional VSR signal processing: 'delay-and-add'). Note particularly the decline in velocity selectivity as the matched velocity increases. This is shown by the increasing width of the peaks as the peak position moves to a higher velocity and eventually leads to the absence of a peak in the 90 m/s curve (Fig 8(a)). This is an artefact of the method and when interpolation (1 to 8) is introduced (Fig 8(b)), the peak is clearly visible, albeit at an incorrect velocity. By comparison, consider the plots shown in Figs 8(c) and (d) which are the outputs from the ANN structure shown in Fig 5. In Fig 8(c), the ANN was trained using a complete AP derived from TMAP1 while in Fig 8(d) the target was a rectangular pulse derived from TMAP1 as described above. The improvement in the response is dramatic, both in terms of selectivity (the narrowness of the response) and the accuracy of the detected velocities. This is especially true for the curves shown in Fig 8(d). Quantitatively, calculating the velocity Q factor (Q_v) discussed earlier, for the curves in Fig 9 [1] – [3], for the 50 m/s case, the comparative values are 1.2 (delay-and-add: both cases); 7.1 (ANN with AP target) and 12.5 (ANN with pulse target).

The ability to discriminate the direction of travel of the AP through the MEC was also tested and it was found that for a 90m/s trained system, the maximum normalised response to an AP travelling in the opposite direction to the training was 0.1. For a 20m/s trained system, the maximum normalised response was just 0.02.

B. The addition of noise.

The tuning curves shown in Fig 8 are ideal in the sense that they were generated using noiseless training data and a noiseless target. A practical system is required to reconstruct the original signal in the presence of noise and/or partial or incomplete data (generalisation) and so the network was retrained with data to which noise had been added. Six sets of 116 (= 696) APs were generated by the synthesiser with a range of conduction velocities from 4 m/s to 120 m/s in steps of 1 m/s, each set having a different SNR value (0.1, 1, 5, 10, 25, 50, 100).

The trained network was tested using noisy input data and the results are expressed as the tuning curves shown in Fig 9, for SNRs of 0.1 and 1. The figure compares the effect of the noise on the interpolated delay-and-add system and on the ANN trained with both AP and pulse targets. Comparing these results with the noiseless ones in Fig 8 it is clear that the delay-and-add method is more susceptible to noise than the ANN. This is seen in the increase in relative response to non-matched APs which makes the matched APs less easy to distinguish. For the SNR = 1 example, Q_v = 1.1 for delay-and-

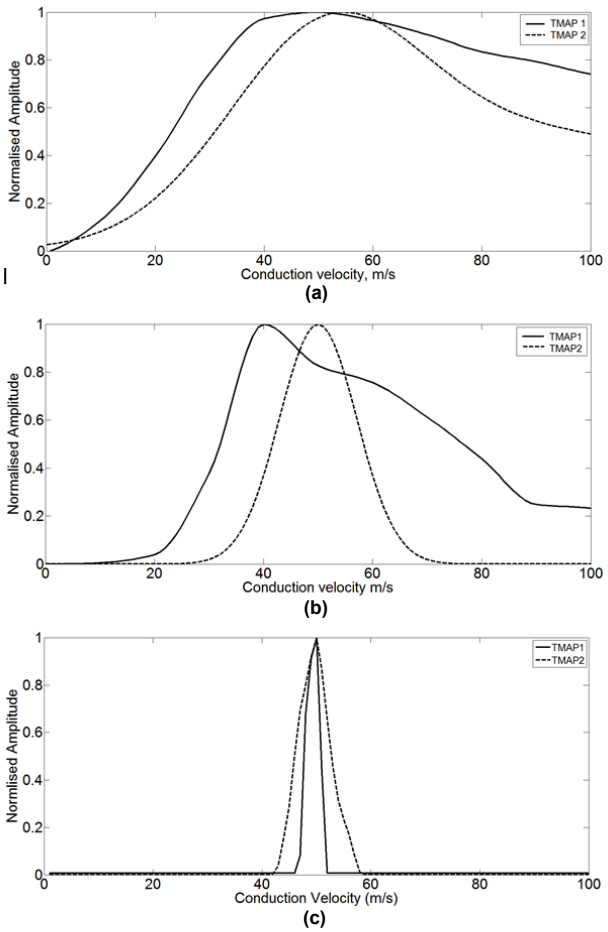

Fig. 10. Tuning curves showing the response of the systems to APs derived from different TMAPs. In the case of the ANN, the training targets were generated using TMAP1 while the inputs were derived from TMAP2 (see section III.C (The effect of varying the TMAP function) for definitions of the TMAPs). The comparisons are made using an AP propagation velocity of 50 m/s and there was no additive noise. Plot (a) shows the effect of switching TMAPs on the standard delay-and-add type classification while plots (b) and (c) consider the effects of this process on the ANN with AP and pulse training respectively. Note that in all cases the change in input signal results in a decrease in Qv and for delay-and-add and the ANN with AP training there is an additional error in centre velocity v0. However, for the ANN with a pulse target, both these errors are visibly reduced.

add, 3.8 for the ANN with the AP target and 10.0 for the ANN with the pulse target. For the case with SNR = 0.1, the corresponding values of Q_V are 0.6, 2.3 and 6.3, respectively. In addition, it should be noted that in the delay-and-add case, the centre velocity increases with the addition of noise whilst the ANN is fairly stable in this respect.

C. *The effect of varying the TMAP function*

The simulations presented so far have been based on the use of the same AP for both input and training. The AP used was derived from TMAP1-see Section II.B.3 (ANN training method). In practice a velocity classifier is required to select APs derived from any TMAP of each velocity without re-training and in real-time. In this section, the effect of varying the form of the TMAP is examined-i.e. the ability of the system when trained using one TMAP function to classify successfully APs generated from a second TMAP. The second TMAP, which was also examined as representing mammalian electroneurogram in [2], has the following parameters: A = 7.44 x 10^{-11}, $B = 10^4$ and $n = 3$. As noted in [2] and shown in Fig. 2, the two TMAPs are significantly different from one another.

The results of the comparisons are shown by the three sets of tuning curves in Fig 10 where the dotted curves represent TMAP1 and the solid curves TMAP2. A single velocity of 50 m/s was considered and there was no additive noise. For the delay-and-add case (top plot) it is noticeable that both the velocity selectivity (Q_v = 1.44 for TMAP1 and 0.63 for TMAP2) and the centre velocity (55 m/s and 50 m/s respectively) are reduced for TMAP2 in comparison to TMAP1 due to sampling effects [2]. The middle and lower plots show how the performances of the ANN, trained using the two targets described above are affected by a change in TMAP function. The networks were trained with a noiseless version of TMAP1 as a template and were then tested with TMAP2 as an input. With the AP target the centre velocity (v_0) is reduced from 50 m/s to about 40 m/s but for the pulse target v_0 does not change appreciably. In addition, the velocity selectivity is reduced for both training methods but much less for the version of the ANN with the pulse target. It is clear that the ANN trained with a rectangular pulse outperforms the other methods most strikingly and is the training method of choice in this application.

IV. Discussion

A. *The need for the new methods proposed in this paper*

The *delay-and-add* system in its current form was first proposed as a method to provide velocity spectral analysis of multi-channel propagating AP in 2004 [1]. Its properties have subsequently been discussed [1]-[6]. Although it provides a very robust approach to the problem of velocity spectral analysis, there are a number of key weaknesses, as noted in section II.B.1 (Conventional VSR signal processing: 'delay-and-add'). In particular, both the *velocity selectivity* and *velocity resolution* are limited, especially at high velocities and the various methods that have been proposed to deal with these problems have met with limited success.

B. *Choice of ANN and its effectiveness in this application*

In order to achieve more effective velocity spectral analysis than is possible using the delay-and-add method, a non-linear approach has been adopted here using, specifically, a *time-delay neural network* [18], [21]. The choice of this type of network was motivated by clear analogies between speech and time-series prediction and multichannel VSR, when the latter is treated as a velocity *classification* process. In addition, since a time-delay neural network requires *supervised learning*, once trained it can run in real-time, which is a significant advantage in this application. Note that all of these processes (i.e. rather than some of them) could have been carried out in MATLAB but it was decided to use real amplifiers and filters so as to be as close as possible to a final system suitable for implantation.

TABLE II
DEVICE UTILIZATION SUMMARY AND POWER CONSUMPTION

Method	Parameter	Result
Delay-and-add	Total equivalent gate count for design	867,187
	Current consumption	19 mA
	Total Power consumption (measured)	22.8mW
	Total power consumption (estimated)	22.23mW
ANN	Total equivalent gate count for design	1,563,624
	Current consumption	38 mA
	Total Power consumption (measured)	45.6mW
	Total power consumption (estimated)	48.94mW

The performance of the ANN shown in Figs 9 and 10 significantly outperforms a delay-and-add system having the same number of channels in terms of both velocity selectivity (Q_v) and resolution (R_v). This improvement can be explained as follows. A delay-and-add network of the type shown in Fig 3 can be regarded as an array of N (N is 9 in this case) FIR filters each having a single weight of fixed value (unity). By contrast the N filters that form the basis of the ANN described here each have 40 weights, all independently programmable, offering many more degrees of freedom for shaping the overall response than is possible for simple delay-and-add. When used in combination with a nonlinear transfer function, a very effective velocity classifier is obtained. It should also be noted that when the network is trained using a rectangular pulse derived from the target AP as described in section II.B.3 (ANN training method), a further, very significant increase in selectivity is obtained. There are two main reasons for this. Firstly, since the AP is replaced by a pulse whose width is less than the AP itself, there is inevitably an increase in selectivity [2]. Secondly, since in the training process noise is only fed back when the pulses (i.e. the training data and the target) are non-zero, the noise power will be significantly less than when the complete AP is used, increasing the accuracy of the training algorithm.

The high selectivity and robustness of the ANN approach offers considerable promise for future therapeutic applications. For example, the two main bladder afferents in humans (*stretch* and *tension*) have propagation velocities of 44 and 38 m/s respectively [24]. In order to separate these using VSR, we require Q_v to be about 41m/s divided by 6m/s or about 7. The data in Fig 10 suggests that this is possible for the pulse-trained ANN even in the presence of significant levels of noise.

C. Hardware considerations

Table II shows the device utilization summary and estimated power consumption for both approaches. Compared with the *delay-and-add* system, the ANN requires approximately double the number of gates and double the power consumption. However this increase should be considered in the context that our design is implemented using FPGA[1], which is well known to have significantly higher power consumption than a comparable custom device of the type that would be required in an implantable system. For example we estimate that moving to a (conservative) 0.18um process would be enough to counteract the impact of the additional processing in the ANN-based system.

In an implantable system based on the type of ANN described in this paper the only change needed to detect different velocities is a change in the weights. The system is therefore adaptable to different situations and applications. For example whilst a complete set of ANNs could be constructed to detect APs with propagation velocities in the range 10 – 120 m/s with, say, 1 m/s resolution, this would not be necessary in a system designed to detect human bladder afferents which occur in the range 30 – 50 m/s. this allows considerable flexibility in the system design in terms of size and power consumption. Furthermore, in all these instances the weights required to realize ANNs sensitive to particular velocities can be generated off-line (i.e. unsupervised) and simply downloaded from a database as required.

REFERENCES

[1] Taylor J, Donaldson N, & Winter J, (2004). "Multiple-electrode nerve cuffs for low velocity and velocity-selective neural recording". Med. & Biol. Eng. & Comput., 42 (5), pp. 634-43..

[2] Taylor, J., Clarke, C., Schuettler, M. and Donaldson, N,(2012). " The theory of velocity selective neural recording: a study based on simulation". Med. & Biol. Eng. & Comput., 42 (5), pp. 309-318 , 2012.

[3] Donaldson N, Rieger R, Schuettler M & Taylor J (2008). "Noise and Selectivity of Velocity-Selective Multi-Electrode Nerve Cuffs". Med. & Biol. Eng. & Comput., 46 (10), 1005-1018.

[4] Rieger R, Schuettler M, Pal D, Clarke C, Langlois P, Taylor J & Donaldson N (2006). "Very low-noise ENG amplifier system using CMOS technology". IEEE Trans Neural Syst Rehabil Eng. 14(4): 427-37.

[5] Yoshida K, Kurstjens G, & Hennings K (2009). "Experimental validation of the nerve conduction velocity selective recording technique using a multi-contact cuff electrode". Medical Engineering & Physics 31: 1261-1270.

[6] Rieger, R, Taylor, J & Clarke, C (2012). "Signal Processing for Velocity Selective Recording Systems Using Analogue Delay Lines". in Proc. ISCAS, May 2012, pp. 2195 - 2198.

[7] Clarke C, Xu X, Rieger R, Taylor J & Donaldson N (2009)." An implanted system for multi-site nerve cuff-based ENG recording using velocity selectivity". Analog Integrated Circuits and Signal Processing, 58 (2), pp. 91-104.

[8] Haugland, M et al (1997). "Restoration of lateral hand grasp using natural sensors". Artificial Organs 21 (3): pp.250-253.

[9] Hansen, M., Haugland, M. K., & Sepulveda, F. (2003). "Feasibility of using peroneal nerve recordings for deriving stimulation timing in a foot drop correction system". Neuromodulation 6(1), pp.68–77.

[10] Hoffer, J (1990). "Techniques to study spinal cord, peripheral nerve and muscle activity in freely moving animals." In: Neuromethods, 15: Neurophysiological Techniques: Applications to Neural Systems. Pp.65-145, Boulton, A.A., Baker, G.B., Vanderwolf, C.H. (eds), The Humana Press Inc., Clifton, NJ.

[1] The exact device used was a Xilinx Spartan 3E: XC3S1200E-5FG320C.

[11] M. Schuettler, N. Donaldson, V. Seetohul, and J. Taylor (2013), "Fibre-selective recording from the peripheral nerves of frogs using a multi-electrode cuff.," Journal of Neural Engineering, vol. 10, no. 3, pp. 1-11.

[12] Nielsen, T. N., Struijk, J., Harreby, K. R., & Sevcencu, C. (2013), "Early detection of epileptic seizures in pigs based on vagus nerve activity", In Pons, J. L., Torricelli, D., & Pajaro, M. (Eds.), Converging Clinical and Engineering Research on Neurorehabilitation. (pp. 43-47). Springer. (Biosystems and Biorobotics, Vol. 1).

[13] Rindos A., Loeb G., Levitan H. (1984). "Conduction Velocity Changes along Lumbar Primary Afferent Fibres in Cats", Experimental Neurology, Vol. 86, pp. 208-226.

[14] Krarup C., Loeb G. (1988) "Conduction Studies in Peripheral in Cat Nerve Using Implanted Electrodes: I Methods and Findings in Controls". Muscle and Nerve, Vol. 11, pp. 922-932.

[15] Stein R., Charles D., Davis L., Jhamandas J., Mannard A. & Nichols T. (1975) "Principles underlying new methods for chronic neural recording." *Can J Neurol Sci.* 2(3), pp.235-44.

[16] Stieglitz T., Beutel H., Schuettler M, et al. (2000) "Micromachined Polyimide-Based Devices for Flexible Neural Interfaces", *Biomed. Microdevices*, Vol: 2, No: 4, pp.283-294.

[17] Choi C, Carpaneto J, Lago N, Kim J, Dario P, Navarro X, Micera S, (2007) "Classification of Afferent Signals Recorded with a Single Cuff Electrode". 29th Annual International Conference of the IEEE Engineering in Medicine and Biology Society (EMBC), Lyon, France.

[18] Waibel, T. Hanazawa, G. Hinton, K. Shikano, and K. Lang, (1989) "Phoneme recognition using time-delay neural networks" *IEEE Trans. Acoustics, Speech, Signal Processing*, vol. 37, pp. 328–339..

[19] Al-Shueli A. Clarke C.T. Taylor J.T. (2012) "Simulated Nerve Signal Generation for Multi-electrode Cuff System Testing," International Conference on Biomedical Engineering and Biotechnology (iCBEB), pp.892-896, Macau, China.

[20] Pflaum, C.; Riso, R.R.; Wiesspeiner, G., "Performance of alternative amplifier configurations for tripolar nerve cuff recorded ENG," Engineering in Medicine and Biology Society, 1996. Bridging Disciplines for Biomedicine. Proceedings of the 18th Annual International Conference of the IEEE , vol.1, no., pp.375,376 vol.1, 31 Oct-3 Nov 1996

[21] E. A. Wan, (1993), "Time series prediction by using a connectionist network with internal delay lines," in *Time Series Prediction: Forecasting the Future and Understanding the Past*, A. S. Weigend and N. A. Gershenfeld, Eds. Reading, MA: Addison-Wesley. .

[22] Charalambous C. (1992),"Conjugate gradient algorithm for efficient training of artificial neural networks," IEEE Proceedings, vol. 139, no. 3, pp. 301–310,

[23] Vogl T. P., Mangis J. K., Rigler A. K., Zink, W. T. and Alkon, D. L. (1988), "Accelerating the convergence of the backpropagation method," Biological Cybernetics, vol. 59, pp. 256-264.

[24] Schalow G., Zäch G. and Warzok R. (1995), "Classification of human peripheral nerve fibre groups by conduction velocity and nerve fibre diameter is preserved following spinal cord lesion", Journal of the Autonomic Nervous System vol 52 pp125-150.

Assad I. Al-Shueli Received BSc. degree in Electrical Engineering in 1998 and MSc. degree in Electronics and Communication in 2001 from Al-Mustansiriya University in Iraq . In 2001 – 2009, he worked at University of Diyala and University of Thi-Qar in Iraq as a lecturer. In July 2009, he started his research with the Microelectronics and Optoelectronics research group as PhD student in the Department of Electronic and Electrical Engineering at the University of Bath. He has published 4 papers in conferences and journals.

Christopher T. Clarke received a B.Eng.degree in Engineering Electronics and a Ph.D. degree in Computer Science from the University of Warwick in 1989 and 1994, respectively. From 1994 to 1997, he lectured at Nanyang Technological University in Singapore where he was a cofounder of the Centre for High Performance Embedded Systems (CHiPES). He joined the Microelectronics and Optoelectronics research group in the Department of Electronic and Electrical Engineering at the University of Bath in March 2003. He is a member of the Centre for Advanced Sensor Technologies (CAST). Dr Clarke is a member of the IET and has published in excess of 40 papers in conferences and journals.

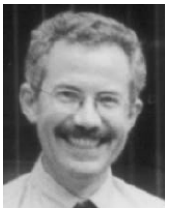

Nick Donaldson studied Engineering and Electrical Sciences at Cambridge University. Since 1992, he has been Head of the Implanted Devices Group at University College London. He has been Principal Investigator for many projects related to implanted devices and functional electrical stimulation. He is a Professor in the University. Dr Donaldson's research interests now includes the development of implanted devices that use natural nerve signals as inputs; stimulators of nerve roots; the use of electrical stimulation for recreational exercise of paralysed legs; and methods to encourage functional neurological recovery after injury.

John Taylor received the BSc and PhD degrees from Imperial College, London University, London, UK, in 1973 and 1984, respectively. In 1984–1985, he worked in the Department of Electrical Engineering, University of Edinburgh, Scotland. He joined the Department of Electronic and Electrical Engineering at University College London in 1985 and subsequently, in 2002, the Department of Electronic and Electrical Engineering at the University of Bath, Bath, UK, where he holds the position of Professor of Microelectronics and Optoelectronics and Director of the University Centre for Advanced Sensor Technologies. His research interests are in the field of analogue circuit and system design, including communication systems and low-power implantable systems for biomedical and rehabilitation applications. Professor Taylor has published more than 140 technical papers in international journals and conferences and has co-edited a handbook on filter design.